ICRC'07 Mérida, México

# Observation of the ULIRG Arp 220 with MAGIC

V. VITALE[1], E. DOMINGO-SANTAMARÍA[2], D.F. TORRES [2 3], M.PERSIC[4], FOR THE MAGIC COLLABORATION
[1]*Dip.Fisica, Universitá di Udine, Udine, Italy*
[2]*Institut de Física d'Altes Energies, Barcelona, Spain*
[3]*ICREA & Institut de Ciencies de L'Espai (IEEC-CSIC), Barcelona 08193, Spain*
[4] *Istituto Nazionale di Astrofisica-Oss.Astron.di Trieste, Trieste, Italy*
*vitale@fisica.uniud.it*

**Abstract:** The ultra-luminous infra red galaxies (ULIRGs) have an enhhanced starburt rate which might be related to a large emission of very high energy gamma rays. Arp 220 is the nearest ULIRGs (72Mpc) and a well studied object. This source was observed with the stand alone imaging atmospheric Cherenkov telescope MAGIC for more than 15 hours on-source. No significant gamma ray excess was detected during the observations. The first upper limits to the very high energy gamma ray flux were obtained, with an analysis energy threshold of 160 GeV. The analysis results will be reported and compared to theoretical expectations.

## Introduction

A large amount of stellar UV photons are emitted within starburst galaxies, and reprocessed to infrared (IR) radiation by local abundant dust. Therefore these galaxies show a large IR luminosity. Luminous and Ultra-Luminous IR galaxies (LIRGs and ULIRGs) are those ones having $\log(L_{IR}/L_{sun}) > 11$ and 12 respectively [20]. The high rate of supernovae and the numerous young massive stars, coupled to the high density of interstellar gas within these type of galaxies might enhance the $\gamma$ ray galactic output, of orders of magnitude, with respect to the normal galaxies ([22],[23]).

LIRGs are the dominant population of galaxies at z<0.3, and ULIRGs are the most luminous local objects. Often the ULIRGs are recent galaxy mergers. As an effect of these galaxies collisions most of the gas of the two objects is attracted by a common center of gravity. Then the gas is concentrated in regions with extension less than 1 kpc, in which an intense starburst is started ([21], [18]). The inner active regions of the ULIRGs have high density molecular gas, associated with large star formation rate and cosmic ray densities. ([13],[14]). Therefore the ULIRGs are candidate $\gamma$ ray sources.

Up to now LIRGs and ULIRGs were not detected as $\gamma$ ray emitters. The EGRET detector on board of the CGRO satellite, working in the 30 Mev - 10 GeV energy range, did not detect any of them. Upper limits were obtained for M82 and NGC 253 and for many LIRGs ([24],[9]). An upper limit of 1.9 $10^{-12}$ ph cm$^{-2}$ s$^{-1}$ above 300 GeV was reported by the HESS collaboration for NGC 253 [2] . The first bound on the very high energy $\gamma$ ray emission from Arp 220 [3] was obtained with the MAGIC telescope and is discussed in the following.

## Observations and Results

Observations of Arp 220 were performed with the MAGIC ([4],[10]) stand alone Imaging Atmospheric Cherenkov Telescope (IACT), which is located on the Canary Island La Palma (28.8°N, 17.8°W, 2200 m a.s.l.). MAGIC is currently the IACT with the largest dish, with a diameter of 17 m. It has a segmented mirror with parabolic shape and a f/D of 1.05. The hexagonal MAGIC camera

Table 1: Number of excess and background events and the corresponding significance and upper limits obtained from the Arp 220 analysis

| SIZE bin (phe) | Average Energy (GeV) | HADR. cut | ALPHA cut (°) | excess events | bckg events | $N_\sigma$ ($\sigma$) | Crab rate ($\gamma$/hr) | $3\sigma$ Upp. Limit $10^{-14}$ (ph cm$^{-2}$ s$^{-1}$ GeV$^{-1}$) |
|---|---|---|---|---|---|---|---|---|
| 200-400 | 160.7 | 0.20 | 10.0 | 295 | 8343 | 2.3 | 171.3 | 80.14 |
| 400-800 | 273.6 | 0.20 | 8.75 | 51 | 2873 | 0.7 | 182.8 | 7.89 |
| 800-1600 | 462.7 | 0.16 | 7.50 | -62 | 707 | -1.8 | 90.2 | 1.00 |
| 1600-3200 | 773.3 | 0.20 | 6.25 | 7 | 370 | 0.3 | 81.1 | 0.40 |
| 3200-6400 | 1351.8 | 0.18 | 6.25 | 22 | 132 | 1.4 | 33.6 | 0.18 |

is composed by 576 hemispherical photomultipliers and has a field of view (FOV) of 3.5°.

The photomultiplier (PMT) analog signal is transmitted to the acquisition electronics with optical fibers. The detector is triggered when at least four neighbouring pixels register a signal above a given threshold.

The $\gamma$ ray point-spread-function (psf) of the telescope is better than 0.1° and changes with the energy. The energy resolution of MAGIC is about 20% and the trigger and analysis energy thresholds are 50 and 60 GeV respectively.

Arp 200 ((J2000) $\alpha$ = $15^h$ $34^m$ $57.21^s$, $\delta$ = 23° 30' 09.5") is visible with zenith angle lower than 20° from La Palma. The source was observed from May to June 2005, with an exposure of 15.78 hours. After the rejection of runs affected by bad atmospheric conditions and low quality data, 15.4 hours of exposure was left for the analysis. Observations were performed in the so-called ON/OFF mode. From the off source observations it is possible to measure the cosmic ray events background. For more details see [11]

The data analysis was carried out using the standard MAGIC analysis and reconstruction software [8], the first step of which involves the calibration of the raw data [15]. After calibration, image cleaning tail cuts of 10 photoelectrons (phe) for image core pixels and 5 phe (boundary pixels) have been applied. These tail cuts are accordingly scaled for the larger size of the outer pixels of the MAGIC camera. The camera images are parameterized by image parameters [16]. In this analysis, the Random Forest method (see [6], [7]) for a detailed description) was applied for the $\gamma$/hadron separation.

The source position-independent image parameters SIZE, WIDTH, LENGTH, CONC [16] and the third moment of the phe distribution along the major image axis were selected to parameterize the shower images. After the training, the Random Forest method allows to calculate for every event a parameter, the HADRONNESS, which is a measure of the probability that the event is not $\gamma$-like. The $\gamma$-sample is defined by selecting showers with a HADRONNESS below a specified value, which is optimized using a sample of Crab data which has been processed with the same analysis stream. An independent sample of Monte Carlo $\gamma$-showers was used to determine the cut efficiency.

In Figure 1 the distributions of the ALPHA parameter after data selection are shown, as function of the SIZE parameter, which is roughly proportional to the events energy. No significant events excess is found at any energy. More details on the selection results are shown in Table 1, where the results are also compared with those obtained from a sample of observations of Crab Nebula. Therefore the upper limits to the differential flux of gamma ray from the source were calculated, using the method by [19]

## Conclusions

With this observation the first upper limits to the differential flux of very high energy gamma rays

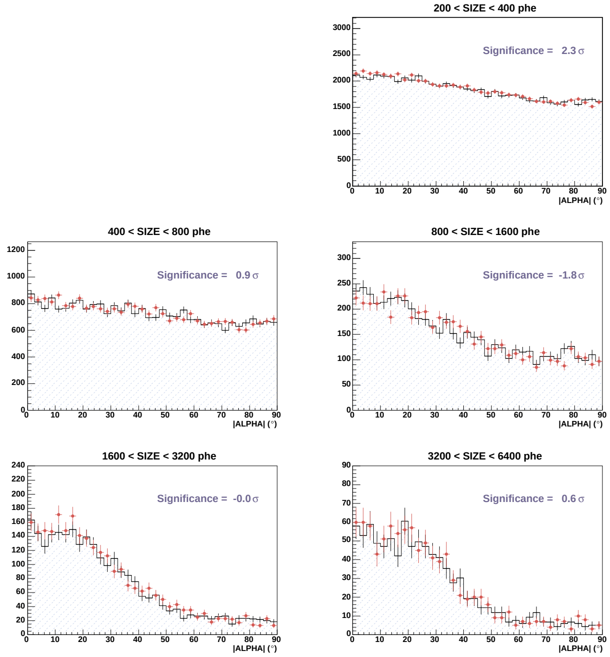


Figure 1: Distributions of the ALPHA image parameter for the Arp 220 data, in bins SIZE. The SIZE parameter is roughly proportional to the gamma ray candidate energy

from the ULIRG Arp 220 was obtained, in the energy range from 160 GeV to 2 TeV. When compared with theoretical predictions of $\gamma$ ray fluxes from Arp 220 these upper limits are one order of magnitude above the models.

The theoretical curves, which are shown in Figure 2, are the result of a multiwavelength modeling discussed by [24], and [25]. From the proton steady state population the computation of the secondary $e^{\pm}$ proceeds considering knock-on interactions and decay of charged pions. The lepton population is let to evolve to its steady state, computing the energy losses by synchrotron emission, ionization, bremsstrahlung, inverse Compton, and adiabatic expansion, and their confinement timescale. The radio spectrum is evaluated from the steady electrons synchrotron emission, modulated by free-free absorption. Infrared emission from dust is also simulated to describe the observational data. These photons are the seed of inverse Compton process. Once the multiwavelength spectrum of the object has been reproduced, the high energy $\gamma$-ray emission is evaluated through the decay of neutral pions, and bremsstrahlung and inverse Compton of the steady electron population. Photon absorption is considered to obtain the final predictions of fluxes.

The curves are obtained using the $\delta$-function [1] or Kamae [17] approaches for the proton-proton cross section parameterization. The latter (see the appendix in [12] for a detailed discussion) are the most reliable parameterizations of the proton-proton cross section, which is devoid of the intrinsic problems of extrapolating in [5] formulae to high energies.

In order to reject or confirm the theoretical $\gamma$-ray flux prediction, one need to study fluxes which are one order of magnitude smaller than the reported upper limits. With the instrument sensitivity obtained for this work, one would need an exposure two orders of magnitude larger, in order to achieve this goal. Such an exposure is comparable with a typical IACT duty cycle, i.e. 1000 hours per year.

Arp 220 is the nearest ULIRG and the galaxy with the largest supernova explosion rate observed so

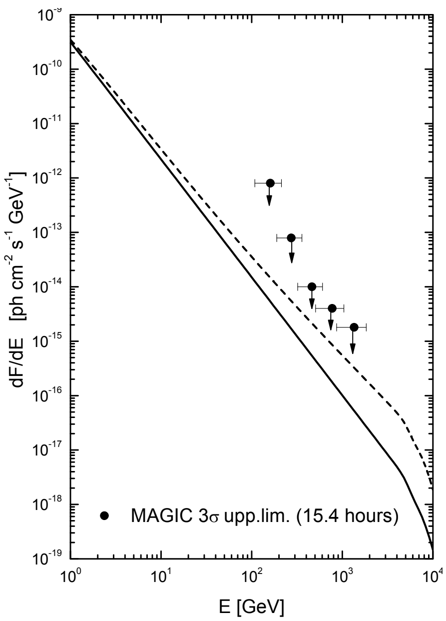


Figure 2: MAGIC upper limits to the differential $\gamma$ ray flux of Arp 220. The curves represent the theoretical predictions: a solid line shows the result using the $\delta$-function ([1]) or Kamae ([17]) approximations for the proton-proton cross section, whereas a dashed line shows the result using the parameterization proposed by [5] extrapolated to high energies. Theoretical curves are from [24],[25]

far. Nevertheless as a consequence of the distance, the galaxy $\gamma$-ray flux is strongly reduced.

MAGIC upper limits are consistent with this interpretation and with the theoretical prediction that results from a complete multiwavelength modeling of the object. The first detection of $\gamma$-rays from starburst regions beyond our galaxy is yet to be achieved.

## Acknowledgements

We would like to thank the IAC for the excellent working conditions at the Observatory de los Muchachos in La Palma. The support of the German BMBF and MPG, the Italian INFN and the Spanish CICYT is gratefully acknowledged. This work was also supported by ETH Research Grant TH 34/04 3 and the Polish MNiI Grant 1P03D01028

## References

[1] F.A. Aharonian et al. . *A&A*, 309:917, 1996.
[2] F.A. Aharonian et al.(HESS coll.). . *A&A*, 442:117, 2005.
[3] J. Albert et al. (MAGIC coll.). . *ApJ*, 658:245, 2007.
[4] C. Baixeras et al. (MAGIC coll.). . *Nucl.Instr.Meth.A*, 518:188, 2004.
[5] S.R. Blattnig et al. . *Phys.Rev.*, 62:094030, 2000.
[6] R.K. Bock. . *Nucl.Insrt.Meth.A*, 516:511, 2004.
[7] L. Breiman. . *Machine Learning*, 45:5, 2001.
[8] T. Bretz et al (MAGIC coll.). . In *Proc. of the 28th ICRC, Tsukuba, Japan*, page 2943, 2003.
[9] A. N. Cillis et al. . *ApJ*, 621:139, 2005.
[10] J.. Cortina et al (MAGIC coll.). . In *Proc. of the 29th ICRC, Pune, India*, pages 5–359, 2005.
[11] E Domingo-Santamaria. *PhD thesis.* (Universitat Autonoma de Barcelona), 2006.
[12] E. Domingo-Santamaria et al. and D. F. Torres. . *A&A*, 444:403, 2005.
[13] Y. Gao et al. . *ApJ Suppl.*, 152:63, 2003.
[14] Y. Gao et al. . *ApJ*, 606:271, 2003.
[15] M. Gaug et al (MAGIC coll.). . In *Proc. of the 29th ICRC, Pune, Japan*, pages 5–375, 2005.
[16] A.M. Hillas. . In *Proc. of the 19th ICRC, La Jolla, Japan*, pages 3–445, 1985.
[17] T. Kamae et al. . *ApJ*, 620:244, 2005.
[18] J. Melnik et al. . *A&A*, 231:L19, 1990.
[19] W. A. Rolke et al. . *Nucl.Instr.Meth.A*, 458:745, 1998.
[20] D. B. Sanders et al. . *ARAA*, 34:749, 1996.
[21] D. B. Sanders et al. . *ApJ*, 325:74, 1998.
[22] D. F. Torres et al. . *ApJ*, 607:L99, 2004.
[23] D. F. Torres et al. . *Rep. Prog. Phys.*, 67:1663, 2004.
[24] D. F. Torres et al. . *ApJ*, 617:966, 2004.
[25] D. F. Torres et al. . *Modern Physics Letters*, page 2827, 2005.